Research Article

Free Vibrations of Beam System Structures with Elastic Boundary Conditions and an Internal Elastic Hinge

Alejandro R. Ratazzi,[1] Diana V. Bambill,[1,2] and Carlos A. Rossit[1,2]

[1] Departamento de Ingeniería, Instituto de Mecánica Aplicada, (IMA), Universidad Nacional del Sur, (UNS),
8000FTN Bahía Blanca, Argentina
[2] Consejo Nacional de Investigaciones Científicas y Técnicas (CONICET), C1033AAJ Buenos Aires, Argentina

Correspondence should be addressed to Diana V. Bambill; dbambill@criba.edu.ar

The study of the dynamic properties of beam structures is extremely important for proper structural design. This present paper deals with the free in-plane vibrations of a system of two orthogonal beam members with an internal elastic hinge. The system is clamped at one end and is elastically connected at the other. Vibrations are analyzed for different boundary conditions at the elastically connected end, including classical conditions such as clamped, simply supported, and free. The beam system is assumed to behave according to the Bernoulli-Euler theory. The governing equations of motion of the structural system in free bending vibration are derived using Hamilton's principle. The exact expression for natural frequencies is obtained using the calculus of variations technique and the method of separation of variables. In the frequency analysis, special attention is paid to the influence of the flexibility and location of the elastic hinge. Results are very similar with those obtained using the finite element method, with values of particular cases of the model available in the literature, and with measurements in an experimental device.

1. Introduction

The study of the dynamic properties of beam systems is very important in structural design as they are the cornerstone for many resistant structures.

The issue is relevant virtually in all fields of engineering: structures composed of beams can resist by virtue of its geometry. Such structures can be found from large scale, such as bridges and buildings located in seismically active regions to microbeam systems used in modern electronic equipment which is subject to vibration environment.

As Laura and his coworkers pointed out [1], many excellent books and technical papers deal with vibrating beam systems, including [2–6].

Many researchers have analyzed the vibration of beam systems. Reference [1] dealt with the determination of the fundamental frequency of vibration of a frame elastically restrained against translation and rotation at the ends, carrying concentrated masses. Reference [7] proposed a hybrid analytical/numerical method to do dynamic analysis of planar serial-frame structures. Reference [8] presented

an elastic- and rigid-combined beam element to determine the dynamic characteristics of a two-dimensional frame composed of any number of beam segments. In his paper, Mei [6] considered the vibration in multistory planar beam structures from the wave vibration standpoint. Reference [9] analyzed in-plane vibrations of portal frames with elastically restrained ends. An approximate solution is obtained by means of a variational method.

In the particular case of L-beam structures, early studies have been done by [10–12]. In 2003, [13] extended the previous papers [12] by relaxing the restrictions on the motion of the open frame. In 2005, [14] determined natural frequencies and mode shapes of elastically restrained L-beams. They applied the separation of variables method for the determination of the exact eigenfrequencies and mode shapes and calculated the eigenvalues numerically by applying the Newton method strategy to the corresponding frequency equation. Reference [15] used a formulation by the Rayleigh-Ritz method together with the introduction of artificial linear and torsional springs for computing the natural frequencies

and modes for the in-plane vibrations of complex planar beam structures.

The presence of an internal hinge in beams has been treated in several papers including [16–22]. Here, we deal with the vibration of L-beams structures assuming an internal hinge in different positions of the structural system.

The two parts of the L-shaped geometry are joined at right angle, with the end of one of them clamped and the end of the other elastically restrained. Figure 1 depicts the structure under study.

Classical structural models do not consider the properties of the connection stiffness, because they are based only on models with pinned or rigid joints. Many authors have studied structures with flexibly connected members as it is known that the behavior of the connection plays an important role in analysis and design. Reference [23] presented a computer-based method for geometrically nonlinear beam system with semirigid beam-to-column connections. Reference [24] studied wooden framed structures; they considered that mechanical connections are recognized as extremely important elements in the aspect of strength and structural safety. Reference [25] studied steel frames and observed that the interstory shears generally increase when the connections stiffness is taken into account. As known, ideal supports used in many structural models do not fit exactly real supports.

In the current presentation it is assumed that the beams are adequately modeled using Euler-Bernoulli theory, so that the effects of shear deformation and rotatory inertia are considered to be small, and they are neglected in the analysis. The cross sections of beam elements have double symmetry (the shear centre and centroid are coincident), so it can be assumed that there is no coupling between bending displacements and torsional rotations.

The beam system is modeled in Mathematica code [26] using the method of separation of variables to obtain the exact values of the natural frequency coefficients.

Finally, numerical results are shown for slender beam systems by considering the effects of different stiffness of the elastic connections. A comparison is made with results obtained by the authors with the finite element method, [27] and with values available in the literature. In addition, some particular cases are also compared with the experimental results of a specially constructed device.

2. Theory

A more realistic model of an L-geometry beam system is presented to analyze the natural vibration problem. The structure under study has elastic restrains at F and a clamped end H as it is shown in Figure 1, with ($\alpha_1 + \alpha_3 = \pi/2$). It is assumed that the elastic internal hinge at P can be located in different positions. The structure has three beam members: FO beam, with length l_1; OP beam, with length l_2; and PH beam, with length l_3. Each of them has uniform properties throughout its length. The influence of the type of connection between beam-elements of the structural system and elastic conditions on the outer edge F is considered in the study. The external end H has a classical clamped condition, while the external end F is supported by two translational springs of stiffness t_w and t_u
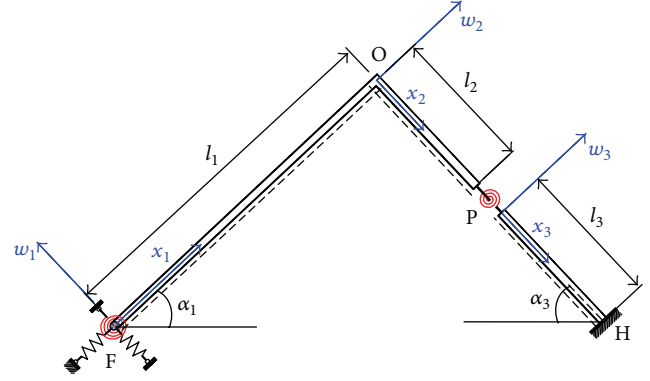

Figure 1: Beam system structure.

and a rotational spring of stiffness r_z, Figure 2(a). At point P, there is an internal hinge, elastically restrained against rotation between beams 2, OP, and 3, PH; this semirigid connection is materialized by a rotational spring of stiffness r_m, Figure 2(b).

The flexural rigidity, the mass density, the length, and the area of the cross section of each beam are E_iI_i, ρ_i, l_i, and A_i, with $i = 1, 2, 3$.

Three coordinate systems are located as shown in Figure 1. Respectively, each coordinate origin is at the point F, O, or P. At abscissa x_i ($0 \leq x_i \leq l_i$) and at any time t: w_i is the flexural displacement in the transverse direction of the beam's neutral axis, $\theta_i = \partial w_i/\partial x_i$ is the section rotation, and u_i is the axial displacement. The deformation of a beam in the x direction is not taken into account. The beams are considered infinitely rigid in the x direction.

The sign convention used for the positive shear force spins an element clockwise (up on the left and down on the right). Likewise the normal convention for a positive bending moment elongates the reference fiber of the beam indicated by the dotted line. Figure 3 shows the sign convention to be employed.

For free vibration, the bending moment and the shear force expressions are

$$Q_i(x_i, t) = E_iI_i \left. \frac{\partial^3 w_i}{\partial x_i^3} \right|_{(x_i, t)},$$

$$M_i(x_i, t) = E_iI_i \left. \frac{\partial^2 w_i}{\partial x_i^2} \right|_{(x_i, t)}. \tag{1}$$

At time t, the kinetic energy of the beams is given by

$$T^* = \sum_{i=1}^{3} \frac{1}{2} \left(\int_0^{l_i} \rho_i A_i \left(\left. \frac{\partial w_i}{\partial t} \right|_{(x_i, t)} \right)^2 dx_i \right)$$

$$+ \frac{\rho_1 A_1 l_1}{2} \left(\left. \frac{\partial u_1}{\partial t} \right|_{(l_1, t)} \right)^2. \tag{2}$$

The last term of the kinetic energy expression is due to the rigid body translation of beam 1 of length l_1. Due to the assumption of infinity axial rigidity, $\partial u_1/\partial t$ at $x_1 = l_1$ is equal to $\partial w_2/\partial t$ at $x_2 = 0$; therefore in (2) the expression $(\partial u_1/\partial t)^2|_{(l_1, t)}$ can also be replaced by $(\partial w_2/\partial t)^2|_{(0, t)}$.
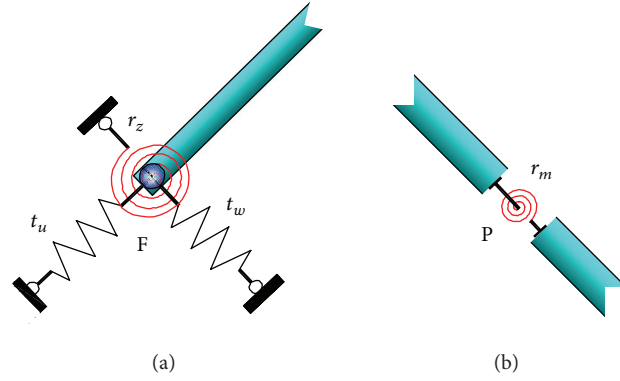
(a) (b)

Figure 2: (a) Elastic boundary conditions at end F; (b) elastic internal hinge at joint P.

On the other hand, the potential energy of the mechanical system is given by

$$U^* = \frac{1}{2}\sum_{i=1}^{3}\left[\int_0^{l_i} E_i I_i \left(\frac{\partial^2 w_i}{\partial x_i^2}\bigg|_{(x_i,t)}\right)^2 dx_i\right]$$

$$+ \frac{1}{2}r_m \left(\frac{\partial w_2}{\partial x_2}\bigg|_{(l_2,t)} - \frac{\partial w_3}{\partial x_3}\bigg|_{(0,t)}\right)^2$$

$$+ \frac{1}{2}r_z\left(\frac{\partial w_1}{\partial x_1}\bigg|_{(0,t)}\right)^2 + \frac{1}{2}t_w(w_1(0,t))^2 \qquad (3)$$

$$+ \frac{1}{2}t_u(u_1(0,t))^2,$$

which involves the work of the elastic constrains. And again due to the assumption of infinity axial stiffness, $u_1(0,t) = u_1(l_1,t) = w_2(0,t)$; therefore in (3) the expression $(u_1(0,t))^2$ can also be replaced by $(w_2(0,t))^2$.

To express equations in dimensionless form, the nondimensional parameter is introduced:

$$X_i = \frac{x_i}{l_i}, \quad \text{with } X_i \in [0,1] \ \forall i = 1,2,3. \qquad (4)$$

The displacements u_i and w_i, and θ_i may be expressed in terms of the dimensionless coordinates as follows:

$$W_i(X_i,t) = \frac{w_i(x_i,t)}{l_i},$$

$$\theta_i(X_i,t) = \frac{\partial W_i}{\partial X_i}\bigg|_{(X_i,t)} = \frac{\partial w_i}{\partial x_i}\bigg|_{(x_i,t)}, \qquad (5)$$

$$U_i(X_i,t) = \frac{u_i(x_i,t)}{l_i}.$$

The characteristics of beam 1 are used as "reference":

$$EI = E_1 I_1, \qquad \rho A = \rho_1 A_1, \qquad l = l_1, \qquad (6)$$

to define the ratios:

$$v_{EI_i} = \frac{E_i I_i}{EI}, \qquad v_{\rho A_i} = \frac{\rho_i A_i}{\rho A}, \qquad v_{l_i} = \frac{l_i}{l}, \qquad (7)$$
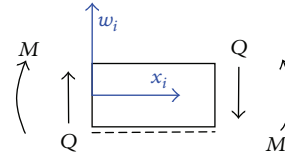

Figure 3: Sign convention for positive transverse displacement (w), shear force (Q), and bending moment (M).

the dimensionless spring stiffness:

$$T_w = t_w\frac{l^3}{EI}, \qquad T_u = t_u\frac{l^3}{EI},$$

$$R_z = r_z\frac{l}{EI}, \qquad R_m = r_m\frac{l}{EI}, \qquad (8)$$

and the dimensionless frequency coefficient:

$$\lambda^4 = l^4\omega^2\frac{\rho A}{EI}, \qquad (9)$$

where ω is the circular natural frequency of the vibrating system in radians per second.

The expression of the energy functional of the system of beams is $J = T^* - U^*$.

Hamilton's principle requires that $\delta\int_{t_a}^{t_b} J dt$ taken between arbitrary intervals of time (t_a,t_b) at which the positions of the mechanical system are known is equal to zero. That means that the system should execute a motion which makes the functional J stationary on the space of admissible functions:

$$\delta\int_{t_a}^{t_b}(T^* - U^*)\,dt = 0, \qquad (10)$$

$$\delta\int_{t_a}^{t_b}(T^* - U^*)\,dt$$

$$= \delta\left\{\frac{1}{2}\rho A l^3\right.$$

$$\times\left\{\int_{t_a}^{t_b}\left[\sum_{i=1}^{3}\int_0^1 v_{\rho A_i}v_{l_i}^3\left(\frac{\partial W_i}{\partial t}\bigg|_{(X_i,t)}\right)^2 dX_i\right.\right.$$

$$+ v_{\rho A_1} v_{l_1} v_{l_2}^2 \left(\left. \frac{\partial W_2}{\partial t} \right|_{(0,t)} \right)^2 \right] dt \right\}$$

$$- \frac{1}{2} \frac{EI}{l} \left\{ \int_{t_a}^{t_b} \left[\sum_{i=1}^{3} \int_0^1 \frac{v_{EI_i}}{v_{l_i}} \left(\left. \frac{\partial^2 W_i}{\partial X_i^2} \right|_{(X_i,t)} \right)^2 dX_i \right] dt \right.$$

$$+ \int_{t_a}^{t_b} R_m \left(\left. \frac{\partial W_2}{\partial X_2} \right|_{(1,t)} - \left. \frac{\partial W_3}{\partial X_3} \right|_{(0,t)} \right)^2 dt$$

$$+ \int_{t_a}^{t_b} R_z \left(\left. \frac{\partial W_1}{\partial X_1} \right|_{(0,t)} \right)^2 dt$$

$$+ \int_{t_a}^{t_b} T_w \left(v_{l_1} \right)^2 \left(W_1 \left(0,t \right) \right)^2 dt$$

$$\left. + \int_{t_a}^{t_b} T_u \left(v_{l_2} \right)^2 \left(W_2 \left(0,t \right) \right)^2 dt \right\} \right\} . \tag{11}$$

Taking into account the boundary conditions at the ends, the compatibility, and equilibrium conditions at the joints between beam elements and applying the procedure of calculus of variations in (10), the following boundary and eigenvalue problem is obtained

$$\left. \frac{\partial^4 W_1}{\partial X_1^4} \right|_{(X_n,t)} + k_1^4 \left. \frac{\partial^2 W_1}{\partial t^2} \right|_{(X_1,t)} = 0,$$

$$\left. \frac{\partial^4 W_2}{\partial X_2^4} \right|_{(X_2,t)} + k_2^4 \left. \frac{\partial^2 W_2}{\partial t^2} \right|_{(X_2,t)} = 0, \tag{12}$$

$$\left. \frac{\partial^4 W_3}{\partial X_3^4} \right|_{(X_3,t)} + k_3^4 \left. \frac{\partial^2 W_3}{\partial t^2} \right|_{(X_3,t)} = 0,$$

with $k_i^4 = (\rho_i A_i / E_i I_i) l_i^4$, $i = 1, 2, 3$.

Consider

$$v_{l_1} W_1 (1,t) = 0, \qquad v_{l_2} W_2 (1,t) = v_{l_3} W_3 (0,t),$$

$$\left. \frac{\partial W_1}{\partial X_1} \right|_{(1,t)} = \left. \frac{\partial W_2}{\partial X_2} \right|_{(0,t)},$$

$$\frac{v_{EI_1}}{v_{l_1}} \left. \frac{\partial^2 W_1}{\partial X_1^2} \right|_{(1,t)} = \frac{v_{EI_2}}{v_{l_2}} \left. \frac{\partial^2 W_2}{\partial X_2^2} \right|_{(0,t)},$$

$$\frac{v_{EI_2}}{v_{l_2}} \left. \frac{\partial^2 W_2}{\partial X_2^2} \right|_{(1,t)} - R_m \left(\left. \frac{\partial W_3}{\partial X_3} \right|_{(0,t)} - \left. \frac{\partial W_2}{\partial X_2} \right|_{(1,t)} \right) = 0,$$

$$\frac{v_{EI_3}}{v_{l_3}} \left. \frac{\partial^2 W_3}{\partial X_3^2} \right|_{(0,t)} - R_m \left(\left. \frac{\partial W_3}{\partial X_3} \right|_{(0,t)} - \left. \frac{\partial W_2}{\partial X_2} \right|_{(1,t)} \right) = 0,$$

$$\frac{v_{EI_1}}{\left(v_{l_1} \right)^2} \left. \frac{\partial^3 W_1}{\partial X_1^3} \right|_{(0,t)} + T_w v_{l_1} W_1 (0,t) = 0,$$

$$\frac{v_{EI_2}}{v_{l_2}^2} \left. \frac{\partial^3 W_2}{\partial X_2^3} \right|_{(1,t)} - \frac{v_{EI_3}}{v_{l_3}^2} \left. \frac{\partial^3 W_3}{\partial X_3^3} \right|_{(0,t)} = 0,$$

$$\frac{v_{EI_2}}{\left(v_{l_2} \right)^2} \left. \frac{\partial^3 W_2}{\partial X_2^3} \right|_{(0,t)} + T_u v_{l_2} W_2 (0,t)$$

$$- k^4 v_{l_1} v_{l_2} W_2 (0,t) = 0, \tag{13}$$

$$\frac{v_{EI_1}}{v_{l_1}} \left. \frac{\partial^2 W_1}{\partial X_1^2} \right|_{(0,t)} - R_z \left. \frac{\partial W_1}{\partial X_1} \right|_{(0,t)} = 0,$$

$$v_{l_3} W_3 (1,t) = 0, \qquad \left. \frac{\partial W_3}{\partial X_3} \right|_{(1,t)} = 0.$$

Using the well-known separation of variables method, solution of (12) is assumed to be of the form:

$$W_1 (X_1,t) = \sum_{n=1}^{\infty} W_{1n} (X_1) T (t),$$

$$W_2 (X_2,t) = \sum_{n=1}^{\infty} W_{2n} (X_2) T (t), \tag{14}$$

$$W_3 (X_3,t) = \sum_{n=1}^{\infty} W_{3n} (X_3) T (t).$$

The functions W_{1n}, W_{2n}, and W_{3n} represent the corresponding transverse modes of natural vibration of each beam member and are given by

$$W_{1n} (X_1) = C_1 \cosh \left(\lambda_n \alpha_1 X_1 \right) + C_2 \operatorname{senh} \left(\lambda_n \alpha_1 X_1 \right)$$
$$+ C_3 \cos \left(\lambda_n \alpha_1 X_1 \right) + C_4 \operatorname{sen} \left(\lambda_n \alpha_1 X_1 \right),$$

$$W_{2n} (X_2) = C_5 \cosh \left(\lambda_n \alpha_2 X_2 \right) + C_6 \operatorname{senh} \left(\lambda_n \alpha_2 X_2 \right)$$
$$+ C_7 \cos \left(\lambda_n \alpha_2 X_2 \right) + C_8 \operatorname{sen} \left(\lambda_n \alpha_2 X_2 \right), \tag{15}$$

$$W_{3n} (X_3) = C_9 \cosh \left(\lambda_n \alpha_3 X_3 \right) + C_{10} \operatorname{senh} \left(\lambda_n \alpha_3 X_3 \right)$$
$$+ C_{11} \cos \left(\lambda_n \alpha_3 X_3 \right) + C_{12} \operatorname{sen} \left(\lambda_n \alpha_3 X_3 \right),$$

where $\alpha_i = v_{l_i} \sqrt[4]{v_{\rho A_i} / v_{EI_i}}$ is a mechanical and geometrical parameter, with $i = 1, 2, 3$, $\lambda_n = \sqrt[4]{l^4 \omega_n^2 \rho A / (EI)}$ is the dimensionless frequency coefficient of mode of vibration n, and $C_1, C_2, \ldots, C_{12}$ are arbitrary constants to be determined.

Replacing expressions (15) in (14) and these ones in (13), a linear system of equations in the unknown constants C_1, $C_2, \ldots, C_{12}$ is obtained.

For a nontrivial solution to exist the determinant of the coefficient matrix in the linear system of equations should be equal to zero and the roots of the transcendental frequency equation are the dimensionless frequency coefficients of the mechanical system in Figure 1.

3. Finite Element Method

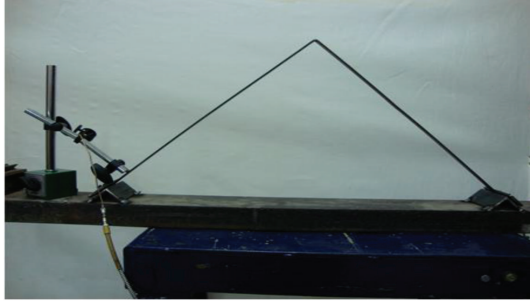The authors solved some numerical examples using the finite element method, using the software ALGOR 23.1 [27].
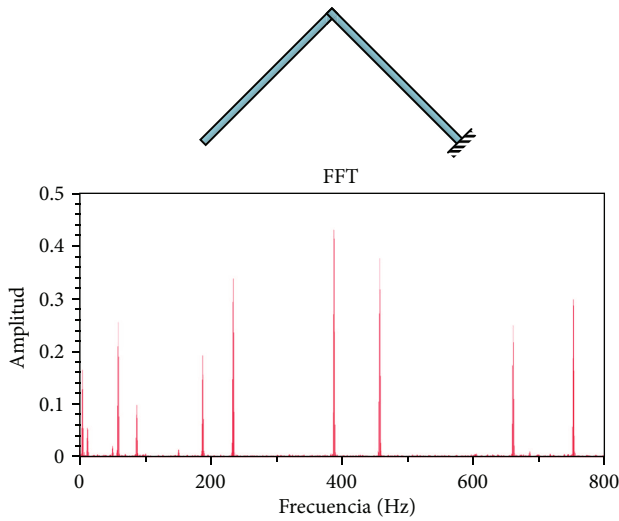
FIGURE 4: Experimental system device; C-C model.

FIGURE 5: Spectrum of the first natural frequency; Case a: F-C model.

FIGURE 6: Spectrum of the first natural frequency; Case b: C-C model.

The three members of the structure are divided into 100 beams elements, respectively, each beam element with three degrees of freedom.

The internal hinge elastically restrained was modeled by a very small beam element, 300 times smaller than the length of the beam. The moment of inertia of the section was varied in order to obtain stiffness values that are equivalent to the stiffness constants of the spring connecting the two sections at location P.

4. Experimental Model

An experimental model was built of steel to compare the results obtained by the analytical and finite element models.

The experimental beam system has two parts of equal length l (see Figure 4). It was tested under two different boundary conditions (clamped and free at $x_1 = 0$) while the other end ($x_3 = 1$) was clamped. The presence of an internal hinge was not considered. The geometry of the structural system is described by $l = l_1 = l_2 + l_3 = 0.50$ m; $A = A_i = 4.064 \times 10^{-5}$ m^2; $I = I_i = 3.468 \times 10^{-11}$ m^4; and the material properties are $\rho = \rho_i = 7870$ kg/m^3 and $E = E_i = 2.1 \times 10^6$ kg/cm^2, with $i = 1, 2, 3$.
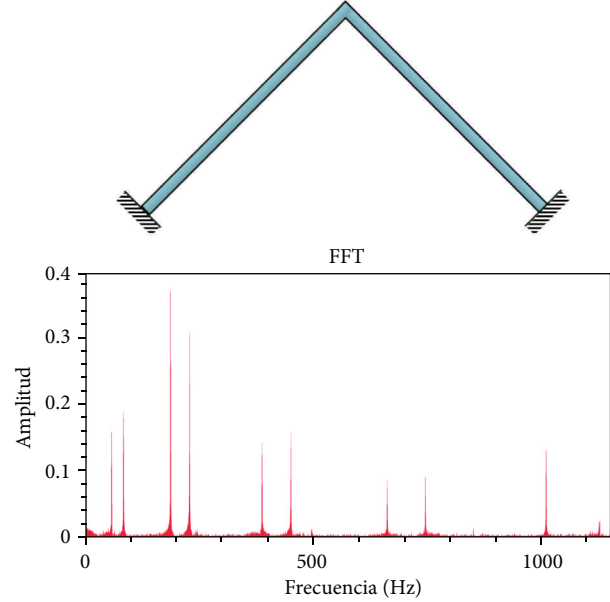
In order to measure the natural frequencies, an optical proximity sensor was used as it is seen in Figure 4.

Figures 5 and 6 show the spectrum of the first ten natural frequencies of the free-clamped (Case a) and the clamped-clamped (Case b) beam systems, respectively.

5. Numerical Results

Frequency coefficients were obtained by the exact analytical solution, with the finite element method, FEM, [27] and with the experimental model.

Table 1 presents the first ten coefficients of natural frequency of vibration of a beam structure with free-clamped boundary conditions without internal hinge, Figure 5.

For the analytical solution the parameters are taken as

$$v_{\rho A_i} = 1, \quad v_{EI_i} = 1, \quad \forall i = 1, 2, 3,$$
$$v_{l_1} = 2v_{l_2} = 2v_{l_3} = 1. \tag{16}$$

The analytical solution for Case a: F-C model, was obtained with $T_u = T_w = R_z = 0$; $R_m \rightarrow \infty$. It is remarkable that for the first ten frequencies, the analytical results are very close to the experimental ones. The analytical results are also compared with previous published ones, [7]. As it can be seen in the table all of them are in excellent agreement.

The exact analytical solution for C-C structure was obtained with $T_u = T_w = R_z = R_m \rightarrow \infty$.

Table 2 shows the first ten coefficients of natural frequency of vibration of the beam structure with clamped-clamped boundary conditions. Again the first ten frequency coefficients obtained by the analytical model are very similar to the experimental model. They also are in excellent agreement with the FEM solution and previous published results [14].

Table 3 shows the frequency coefficients for pinned-clamped L-beams obtained by the analytical procedure and the finite element method. For the analytical solution the spring constants are assigned in two different ways to model the simply supported-clamped system:

(1) $v_{EI_i} = 1$, $v_{\rho A_i} = 1$, for all $i = 1, 2, 3$, $v_{l_2} = v_{l_3} = 1/2$, $T_w \rightarrow \infty$, $T_u \rightarrow \infty$, $R_z = 0$, and $R_m \rightarrow \infty$.

(2) $v_{EI_i} = 1$, $v_{\rho A_i} = 1$, for all $i = 1, 2, 3$, $v_{l_2} = 0.99$, $v_{l_3} = 0.01$, $T_w \rightarrow \infty$, $T_u \rightarrow \infty$, $R_z \rightarrow \infty$, and $R_m = 0$.

The percentage differences between both sets of results are shown in file $|\Delta|\%$. Although both sets of results correspond to a simply supported-clamped system, the small percentage differences, less than 0.7%, are due to the different numerical computational aspects between the analytical models (1) and (2). The results were determined using the Mathematica software [26] with five significant figures.

Table 4 compares the first five natural coefficients of vibration for a free-clamped system with Morales published results [28]. The characteristics of Morales frame are $l_1 = 2.215$ m and $l_2 + l_3 = 4.249$ m, $E_1 I_1 = 0.0147$ Nm^2, $E_2 I_2 = E_3 I_3 = 0.0267$ Nm^2, $m_1 = 6 \times 10^{-3}$ kg/m, and $m_2 = m_3 = 4.5 \times 10^{-5}$ kg/m. For the analytical solution, the parameters are assumed as $l_1 = 2.215$ m, $l_2 = 2.249$ m, $l_3 = 2.000$ m, $v_{l_1} = 1$, $v_{EI_1} = 1$, $v_{\rho A_1} = 1$, $v_{l_2} = 1.0153$, $v_{EI_2} = 1.8163$, $v_{\rho A_2} = 0.0075$, $v_{l_3} = 0.0903$, $v_{EI_3} = 1.8163$, $v_{\rho A_3} = 0.0075$, $T_w = 0$, $R_z = 0$, $T_u = 0$, and $R_m \rightarrow \infty$. It can be verified that our results are in excellent agreement whit those obtained by Morales.

Traditionally, the analysis and design of beam structures have been based on the assumption that the boundary conditions are rigid. The disadvantage of this model is that the flexibility of the real boundary conditions is neglected and therefore the real natural frequencies cannot be obtained.

Thus, we now analyze the case of beam system structure with elastic boundary conditions at edge F and clamped at the other end H, while the internal elastic hinge (at section P) is assumed to have $R_m \rightarrow \infty$. Numerical simulations are carried out to investigate the effect of the rigidity of the boundary conditions on the natural frequencies of the system.

In Figure 7 the effect of rigidity T_u of the translational spring on the frequency coefficients of the structure is shown. It can be seen that the first frequency coefficient λ_1 increases with increasing the value of T_u, from $T_u = 0$, $\lambda_1 = 1.5208$ to $T_u \rightarrow 200$, $\lambda_1 = 3.3762$. For values larger than 200 the fundamental coefficient stays practically the same: $T_u \rightarrow \infty$, $\lambda_1 = 3.3920$. Its increase is of 124%.

The second frequency is 3.3947 for $T_u = 0$ and 4.4566 for $T_u \rightarrow \infty$; its increase is of 31% and the most significant change occurs between $T_u = 200$ and $T_u = 1000$. The higher frequency coefficients exhibit a similar behavior.

From Figure 7 it could be concluded that the first and second frequencies interchange their modal shape for a value of T_u between 100 and 1000. A similar behaviour occurs in the case of third and fourth frequencies for a value of T_u between 1000 and 10000.

Figure 8 shows the effect of T_w on the first natural frequency coefficients. Again it is observed as a matter of course that the natural frequency coefficients increase with the spring constant parameter.
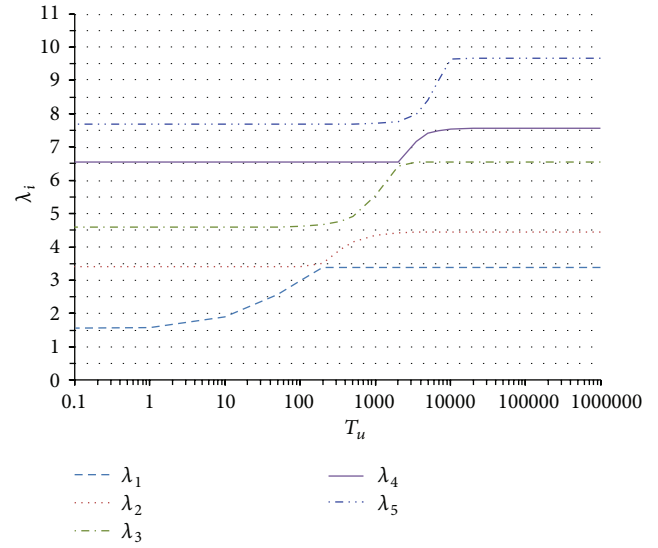

FIGURE 7: Effect of T_u on the first five natural frequency coefficients. $l_2 = l_3$, $v_{l_1} = v_{l_2} = 0.5$, $v_{EI_{(2)}} = v_{EI_{(3)}} = 1$, $v_{\rho A_{(2)}} = v_{\rho A_{(3)}} = 1$, $R_m \rightarrow \infty$, $R_z = 0$, and $T_w \rightarrow \infty$.
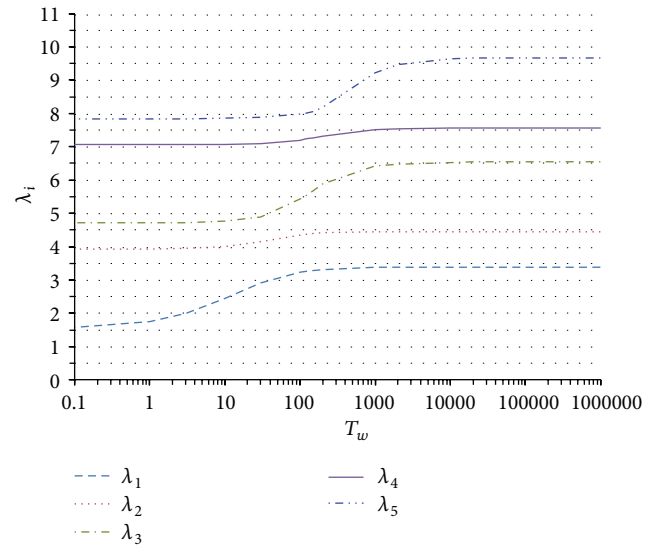

FIGURE 8: Effect of T_w on the first five natural frequency coefficients. $l_2 = l_3$, $v_{l_1} = v_{l_2} = 0.5$, $v_{EI_{(2)}} = v_{EI_{(3)}} = 1$, $v_{\rho A_{(2)}} = v_{\rho A_{(3)}} = 1$, $R_m \rightarrow \infty$, $R_z = 0$, and $T_u \rightarrow \infty$.

Figure 9 shows that the effect of the spring R_z is small.

Table 5 presents the case of a clamped-clamped structure with an elastic joint at $l_2 = 0.5l_1$, and R_m is the constant rigidity of the rotational spring at P that connects the beam members indicated as OP and PH. In this table R_m assumes different values from infinity to zero. It can be seen that all the first frequency coefficients decrease in value, except for λ_4, which practically remains constant.

Table 6 presents the case of a clamped-clamped structure with an elastic connection at P, $l_2 \rightarrow 0$, $l_3 = l_1$. In this table, R_m assumes different values, from $\rightarrow \infty$ to 0. It can

TABLE 1: Comparison of the first ten frequency coefficients $\lambda_n = \sqrt[4]{l^4 \omega_n^2 (\rho A / EI)}$ for L-beams: Case a: F-C.

λ_1	λ_2	λ_3	λ_4	λ_5	λ_6	λ_7	λ_8	λ_9	λ_{10}	
f_1= 4.30	11.90	58.59	86.67	185.38	233.76	386.96	456.54	659.79	751.3	*Experimental, in hertz
1.0811	1.7985	3.9907	4.8537	7.0986	7.9541	10.255	11.139	13.392	14.290	**Experimental, adimensional
1.0820	1.7863	3.9680	4.8031	7.0981	7.9131	10.229	11.034	13.368	14.171	Exact analytical solution
1.0854	1.7903	3.9753	4.8077	7.0956	7.9307	10.225	11.059	13.355	14.191	FEM
1.0880	1.7869	3.9685	4.8021	7.0915	—	—	—	—	—	Lin and Ro, 2003 [7]

*Experimental, in hertz: values f_n were measured in the experimental model (Figure 5).

**Experimental, adimensional: values were obtained from f_n measured values: $\lambda_n = l \cdot \sqrt[4]{(2\pi f_n)^2 (\rho A / EI)}$.

TABLE 2: Comparison of the first ten frequency coefficients $\lambda_n = \sqrt[4]{l^4 \omega_n^2 (\rho A / EI)}$ for L-beams: Case b: C-C.

λ_1	λ_2	λ_3	λ_4	λ_5	λ_6	λ_7	λ_8	λ_9	λ_{10}	
f_1 = 56.76	82.01	182.5	225.88	382.08	448.0	653.08	737.92	992.43	1105.3	*Experimental, in hertz
3.9270	4.7214	7.0432	7.8357	10.190	11.035	13.323	14.162	16.424	17.333	**Experimental, adimensional
3.9229	4.7227	7.0528	7.8249	10.159	10.838	13.310	14.137	16.345	17.178	Exact analytical solution
3.9319	4.7295	7.0613	7.8187	10.158	11.014	13.337	14.152	16.465	17.282	FEM
3.9222	4.7142	7.0376	7.7588	10.007	—	—	—	—	—	Albarracín and Grossi, 2005 [14]

*Experimental, in hertz: values f_n were measured in the experimental model (Figure 6).

**Experimental, adimensional: values were obtained from f_n measured values: $\lambda_n = l \cdot \sqrt[4]{(2\pi f_n)^2 (\rho A / EI)}$.

TABLE 3: Frequency coefficients $\lambda_n = \sqrt[4]{l^4 \omega_n^2 (\rho A / EI)}$ for simply supported-clamped beam system; comparison of results.

λ_1	λ_2	λ_3	λ_4	λ_5	
3.3920	4.4566	6.5383	7.5702	9.6637	Exact analytical solution (1)
3.3943	4.4266	6.5798	7.5666	9.6584	Exact analytical solution (2)
0.07%	0.68%	0.63%	0.05%	0.05%	$\|\Delta\| = ((1) - (2))/(2)$ %(difference)
3.3900	4.4266	6.5292	7.5608	9.6301	FEM

TABLE 4: Non dimensional frequency coefficients $\lambda_n = \sqrt[4]{l^4 \omega_n^2 (\rho A / EI)}$ for free-clamped beam system; comparison of results.

λ_1	λ_2	λ_3	λ_4	λ_5	
1.0301	1.9062	3.5186	5.1798	6.1299	Exact analytical solution
1.0385	1.9198	3.5277	5.1787	6.1156	FEM
1.0229	1.9229	3.5337	5.1844	6.1330	(Morales, 2009 [28]) 12-DOF RRMSSM
1.0229	1.9229	3.5337	5.1844	6.1330	(Morales, 2009 [28]) 60-DOF FEM
1.0229	1.9229	3.5337	5.1841	6.1329	(Morales, 2009 [28]) Analytical

TABLE 5: Effect of R_m on the first five non dimensional frequency coefficients of a C-C system, with an elastic joint at $l_2 = 0.5 l_1$, beam-beam connection.

R_m	λ_1	λ_2	λ_3	λ_4	λ_5	
$\rightarrow \infty$	3.9229	4.7227	7.0528	7.8248	10.1595	Exact analytical solution
500	3.9229	4.7227	7.0528	7.8248	10.1595	
100	3.9145	4.7121	7.0499	7.8248	10.1327	
50	3.9110	4.7082	7.0498	7.8248	10.1086	
20	3.9818	4.6862	7.0436	7.8248	10.0438	
10	3.8614	4.6557	7.0346	7.8248	9.9439	
3	3.7464	4.5724	7.0075	7.8248	9.6334	
1	3.5695	4.4983	6.9776	7.8248	9.3290	
0.5	3.4604	4.4692	6.9631	7.8248	9.2013	
0	3.2662	4.4332	6.9410	7.8247	9.0429	
0	3.2566	4.4247	6.9489	7.8306	9.0501	FEM

TABLE 6: Effect of R_m on the first five non dimensional frequency coefficients of a C-C beam system, with an elastic joint at $l_2 \rightarrow 0, l_3 = l_1$ (exact analytical solution).

R_m	λ_1	λ_2	λ_3	λ_4	λ_5
$\rightarrow \infty$	3.9229	4.7227	7.0528	7.8284	10.1595
500	3.9229	4.7227	7.0528	7.8248	10.1595
100	3.9127	4.6887	7.0340	7.7679	10.1255
50	3.9127	4.6676	7.0340	7.7352	10.1255
20	3.9127	4.6104	7.0339	7.6520	10.1253
10	3.9127	4.5322	7.0336	7.5490	10.1248
3	3.9125	4.3200	7.0327	7.3245	10.1232
1	3.9122	4.1216	7.0304	7.1710	10.1193
0.5	3.9117	4.0365	7.0277	7.1188	10.1157
0	3.9038	3.9296	7.0161	7.0664	10.1059

TABLE 7: Effect of R_m on the first five non dimensional frequency coefficients of a SS-C beam system, with an elastic joint at $l_2 = 0.5l_1$, beam-beam connection (exact analytical solution).

R_m	λ_1	λ_2	λ_3	λ_4	λ_5
$\rightarrow \infty$	3.3920	4.4566	6.5383	7.5702	9.6637
500	3.3920	4.4566	6.5383	7.5702	9.6637
100	3.3903	4.4470	6.5374	7.5692	9.6607
50	3.3883	4.4349	6.5354	7.5687	9.6541
20	3.3821	4.4009	6.5297	7.5672	9.6337
10	3.3723	4.3514	6.5216	7.5651	9.5984
3	3.3318	4.1975	6.4976	7.5585	9.4430
1	3.2548	4.0264	6.4721	7.5509	9.2192
0.5	3.1959	3.9477	6.4602	7.5470	9.1105
0	3.0686	3.8450	6.4432	7.5412	8.9626

TABLE 8: Effect of R_m on the first five non dimensional frequency coefficients of a SS-C beam system, with an elastic joint at $l_2 \rightarrow 0, l_3 = l_1$ (exact analytical solution).

R_m	λ_1	λ_2	λ_3	λ_4	λ_5
$\rightarrow \infty$	3.3920	4.4566	6.5383	7.5702	9.6637
500	3.3920	4.4566	6.5383	7.5702	9.6637
100	3.3884	4.4394	6.5314	7.5314	9.6550
50	3.3851	4.4237	6.5248	7.5123	9.6455
20	3.3757	4.3812	6.5066	7.4501	9.6202
10	3.3614	4.3234	6.4808	7.3751	9.5866
3	3.3107	4.1713	6.4076	7.2219	9.5068
1	3.2413	4.0410	6.3398	7.1283	9.4485
0.5	3.2026	3.9903	6.3120	7.0983	9.4277
0	3.1408	3.9290	6.2768	7.0654	9.4033

be seen that the first, the third, and the fifth frequency coefficients remain practically constant and the second coefficients decrease by 20% and the fourth decrease by 11%.

Table 7 presents the frequency coefficients of a simply supported-clamped structure with an elastic joint at $l_2 = 0.5l_1$.

In the present conditions, the first, the second, and the fifth frequency coefficients decrease in value and the third and fourth remain practically constant.

Table 8 contains the frequency coefficients of a simply supported-clamped beam system with an elastic connection at P, $l_2 \rightarrow 0, l_3 = l_1$. It can be seen that all the frequency coefficients decrease in value between 8% (λ_1) and 3% (λ_5).

Figures 10 and 11 show graphically the variation of first three natural frequency coefficients for various locations of the elastic hinge: $l_2/l \rightarrow 0$ to $l_2/l \rightarrow 1$, with different combinations of R_z, T_w, T_u and R_m. In both figures, it is clear that for the fundamental frequency coefficient the differences in the values of frequencies are not so significant.

6. Conclusions

The model presented in this paper allows studying the effect of the variation in the rigidity of the elastic supports and the elastic joint on the dynamical behavior of the beam system structure. The model enables an efficient, simple, and
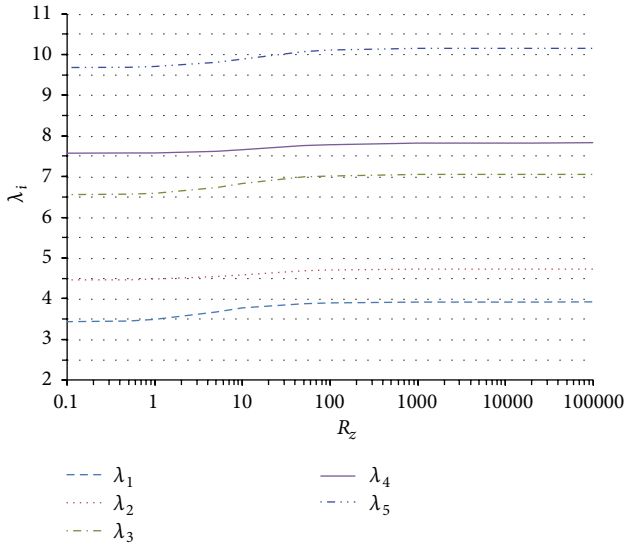
FIGURE 9: Effect of R_z on the first five natural frequency coefficients. $l_2 = l_3$, $v_{l_1} = v_{l_2} = 0.5$, $v_{EI_{(2)}} = v_{EI_{(3)}} = 1$, $v_{\rho A_{(2)}} = v_{\rho A_{(3)}} = 1$, $R_m \to \infty$, $T_w \to \infty$, and $T_u \to \infty$.
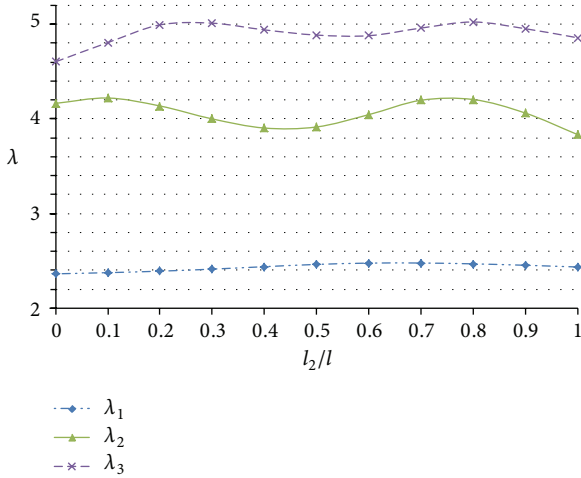

FIGURE 10: Variation of first three natural frequency coefficients with location of the elastic hinge, $l_1 = l_2 + l_3 = l$, $l_2/l \in (0, 1)$, $v_{EI_{(2)}} = v_{EI_{(3)}} = v_{\rho A_{(2)}} = v_{\rho A_{(3)}} = 1$, $R_z = 3$, $T_w = 10$, $T_u = 5$, and $R_m = 2$.

straightforward way of computing natural frequency coefficients for L-Shaped-Structures with many different boundary conditions at simply supported, clamped, free, and elastically restrained. It was observed that the loss of rigidity of the translational springs significantly changes the natural frequency coefficients, especially the fundamental frequency coefficient. The presence of an elastic joint, modeling a beam-beam connection, also implies changes in the natural frequencies when the rigidity is lost.

Although the model with elastic connection and supports does not represent the inherent complexities of real systems such as nonlinearity or damping, it provides conceptual insights regarding the fact that the loss of rigidity can cause significant changes in the dynamic behavior of the structure.
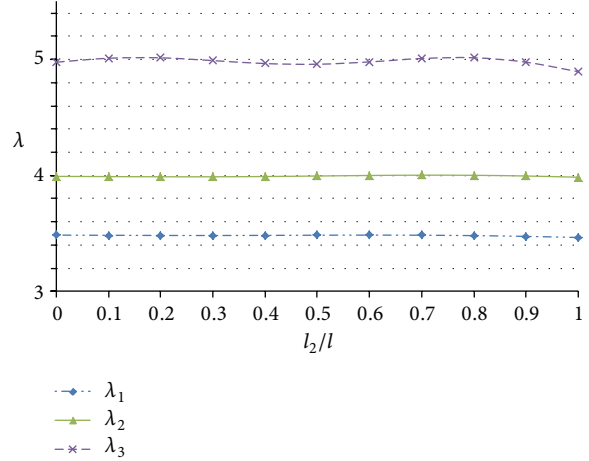

FIGURE 11: Variation of first three natural frequency coefficients with location of the elastic hinge, $l_1 = l_2 + l_3 = l$, $l_2/l \in (0, 1)$, $v_{EI_{(2)}} = v_{EI_{(3)}} = v_{\rho A_{(2)}} = v_{\rho A_{(3)}} = 1$, $R_z = 50$, $T_w = 100$, $T_u = 100$, and $R_m = 20$.

In this sense, this model can be seen as a useful first approach to study the real system. The proposed analytical solution may be applied to include more complicating effects, such as elastic constraints at both ends, more than one internal elastic hinge, and another geometry with $\alpha_1 + \alpha_3 \neq \pi/2$. Finally, it has been demonstrated that an elastic approach constitutes a reliable tool to deal with beam system structures.
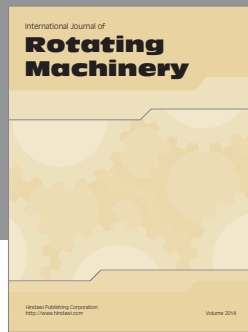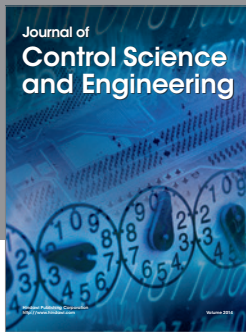
Acknowledgments

References

[1] P. A. A. Laura, B. H. Valerga de Greco, and C. P. Filipich, "In-plane vibrations of frames carrying concentrated masses," *Journal of Sound and Vibration*, vol. 117, no. 3, pp. 447–458, 1987.

[2] G. B. Warburton, *The Dynamical Behaviour of Structures*, Pergamon Press, Oxford, UK, 2nd edition, 1976.

[3] R. Blevins, *Formulas for Natural Frequency and Mode Shape*, Krieger Publishing, Malabar, Fla, USA, 2001.

[4] R. W. Clough and J. Penzien, *Dynamics of Structures*, Computers and Structures, Inc., Berkeley, Calif, USA, 3rd edition, 2004.

[5] S. Timoshenko and D. H. Young, *Vibration Problems in Engineering*, John Wiley & Sons, New York, NY, USA, 5th edition, 1990.

[6] C. Mei, "Wave control of vibrations in multi-story planar frame structures based on classical vibration theories," *Journal of Sound and Vibration*, vol. 330, no. 23, pp. 5530–5544, 2011.

[7] H. P. Lin and J. Ro, "Vibration analysis of planar serial-frame structures," *Journal of Sound and Vibration*, vol. 262, no. 5, pp. 1113–1131, 2003.

[8] J.-J. Wu, "Use of the elastic-and-rigid-combined beam element for dynamic analysis of a two-dimensional frame with arbitrarily distributed rigid beam segments," *Applied Mathematical Modelling*, vol. 35, no. 3, pp. 1240–1251, 2011.

[9] C. P. Filipich and P. A. A. Laura, "In-plane vibrations of portal frames with end supports elastically restrained against rotation and translation," *Journal of Sound and Vibration*, vol. 117, no. 3, pp. 467–473, 1987.

[10] H. Bang, "Analytical solution for dynamic of a flexible L-shaped structure," *Journal of Dynamic*, vol. 19, no. 1, pp. 248–250, 1996.

[11] M. Gürgöze, "Comment on Analytical solution for dynamic analysis of flexible L-shaped structure," *Journal of Guidance, Control and Dynamics*, vol. 21, no. 2, p. 359, 1998.

[12] D. C. D. Oguamanam, J. S. Hansen, and G. R. Heppler, "Vibration of arbitrarily oriented two-member open frames with tip mass," *Journal of Sound and Vibration*, vol. 209, no. 4, pp. 651–668, 1998.

[13] G. R. Heppler, D. C. D. Oguamanam, and J. S. Hansen, "Vibration of a two-member open frame," *Journal of Sound and Vibration*, vol. 263, no. 2, pp. 299–317, 2003.

[14] C. M. Albarracín and R. O. Grossi, "Vibrations of elastically restrained frames," *Journal of Sound and Vibration*, vol. 285, no. 1-2, pp. 467–476, 2005.

[15] H. P. Lee and T. Y. Ng, "In-plane vibration of planar frame structures," *Journal of Sound and Vibration*, vol. 172, no. 3, pp. 420–427, 1994.

[16] R. O. Grossi and M. V. Quintana, "The transition conditions in the dynamics of elastically restrained beams," *Journal of Sound and Vibration*, vol. 316, no. 1-5, pp. 274–297, 2008.

[17] C. Y. Wang and C. M. Wang, "Vibrations of a beam with an internal hinge," *International Journal Structural Stability Dynamic*, vol. 1, pp. 163–167, 2001.

[18] Y. Y. Lee, C. M. Wang, and S. Kitipornchai, "Vibration of Timoshenko beams with internal hinge," *Journal of Engineering Mechanics*, vol. 129, no. 3, pp. 293–301, 2003.

[19] T.-P. Chang, G.-L. Lin, and E. Chang, "Vibration analysis of a beam with an internal hinge subjected to a random moving oscillator," *International Journal of Solids and Structures*, vol. 43, no. 21, pp. 6398–6412, 2006.

[20] M. V. Quintana, J. L. Raffo, and R. O. Grossi, "Eigenfrequencies of generally restrained Timoshenko beam with an internal hinge," *Mecánica Computacional*, vol. 29, pp. 2499–2516, 2010.

[21] R. A. Ratazzi, R. O. Grossi, and D. V. Bambill, "Vibraciones de una estructura aporticada con una rótula intermedia elásticamente restringida contra rotación y traslación," *Mecánica Computacional*, vol. 30, pp. 2499–2516, 2011.

[22] R. A. Ratazzi, D. V. Bambill, and C. A. Rossit, "Vibraciones en porticos con conexiones intermedias elasticas," *Mecánica Computacional*, vol. 31, pp. 2511–2627, 2012.

[23] H. Gorgun, "Geometrically nonlinear analysis of plane frames composed of flexibly connected members," *Structural Engineering and Mechanics*, vol. 45, no. 3, pp. 273–305, 2013.

[24] C. L. O. Santana and N. T. Mascia, "Wooden framed structures with semi-rigid connections: quantitative approach focused on design needs," *Structural Engineering and Mechanics*, vol. 31, no. 3, pp. 315–331, 2009.

[25] A. Reyes-Salazar, M. E. Soto-Lópeza, E. Bojórquez-Morab, and A. López-Barrazab, "Effect of modeling assumptions on the seismic behavior of steel buildings with perimeter moment frames," *Structural Engineering and Mechanics*, vol. 41, no. 2, pp. 183–204, 2012.

[26] Wolfram MATHEMATICA 9 software, Version 9, Copyright 1988–2012.

[27] ALGOR software, Version 23, 01, 2009.

[28] C. A. Morales, "Dynamic analysis of an L-shaped structure by Rayleigh-Ritz substructure synthesis method," *Meccanica*, vol. 44, no. 3, pp. 339–343, 2009.

The Scientific World Journal

Journal of
Control Science
and Engineering

International Journal of
Rotating Machinery

Journal of
Robotics

Advances in
Mechanical Engineering

Journal of
Engineering

International Journal of
Chemical Engineering

International Journal of
Distributed Sensor Networks

Advances in
Civil Engineering

Hindawi

Submit your manuscripts at
http://www.hindawi.com

Advances in
OptoElectronics

VLSI Design

International Journal of
Navigation and Observation

Modelling &
Simulation
in Engineering

Advances in
Acoustics &
Vibration

Active and Passive
Electronic Components

International Journal of
Antennas and
Propagation

Journal of
Sensors

Shock and Vibration

Journal of
Electrical and Computer Engineering